



**UNIVERSITY OF MISKOLC**  
FACULTY OF MATERIAL SCIENCE AND ENGINEERING  
Institute of Metallurgy, Metal Forming and Nanotechnology

\*\*\*\*\*



# **NUMERICAL SIMULATION AND EXPERIMENTAL VALIDATION OF RESIDUAL STRESSES IN A MULTI-PASS WELDED OIL AND GAS PIPE**

A PhD dissertation submitted in the defence process for the degree of  
Doctor of Philosophy

By

**Mahmood Hasan Dakhil ALHAFADHI**

Scientific Supervisors:

**Prof. Dr. György Krállics<sup>†</sup>**  
**Dr. Máté Szűcs**  
**Dr. Sándor Kovács**

**ANTAL KERPELY DOCTORAL SCHOOL OF MATERIALS SCIENCE &  
TECHNOLOGY**

Head of Doctoral School: **Prof. Dr. Zoltán Gácsi**

Institute of Metallurgy, Metal Forming and Nanotechnology  
Faculty of Material Science and Engineering  
University of Miskolc  
Hungary, 2021

## 1. Introduction and literature review

Some industries and applications require pipe welding with dissimilar materials to be joined for chemical, structural, and economic reasons. Combining pipe welding with dissimilar metals allow using of the best properties of each metal. The heat from welding may cause localized expansion, which is taken up during welding by either the molten metal or the shape of welded material parts. After welding, some areas cool and contract more than others, leaving residual stresses. Residual stresses can be tensile or compressive. Tensile residual stresses can be large enough to cause cracking. Despite X-ray diffraction (XRD) being used to measure residual stresses more accurate than other non-directive techniques. Still, there are both physical limitations and practical factors that affect the measurement. Both should be considered. For example, XRD measure only on the surface, and the XRD experimental trials take a long time and require a high cost to capture the optimal welding residual stresses. Numerical simulation is a cost-efficient way to help quantify the reasonable welding parameters and further understand the mechanisms of residual stresses in dissimilar welding pipes. The commonly used validation model, either 2-D or both (2-D and 3-D) are limited almost exclusively to the thermocouple measurement technique. There are also very limited studies on characterising the effect of welding parameters on residual stresses in dissimilar pipe arc welded joints and the approach to reduce the residual stress such as heat input, groove shape, arc welding travel speed, specimen thickness, external mechanical constraints, phase transformation and preheating. Although there are many papers in the literature that used different types of heat source models, these studies are focused only on (Gaussian) and Conical or mostly the Goldak heat source model.

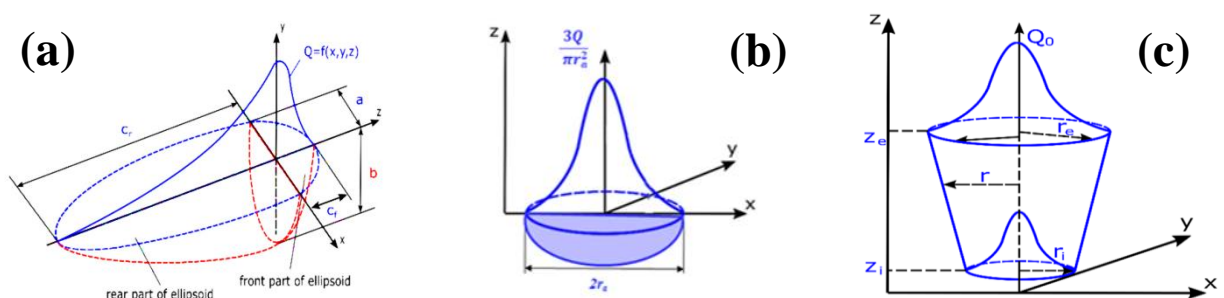


**Figure 1.** (a) Goldak (b) Gaussian (c) Conical heat source model

## 2. Scientific goals

After a careful literature review and identification of the knowledge gap, the following research questions emerged:

- What alternative method can be used for validation of finite element model for pipe arc welding with dissimilar material?

- Is it allowable only to use a two-dimensional model (2-D) for the prediction of residual stresses data for pipe arc welding with dissimilar material?
- What is the effect of different welding parameters on residual stresses in dissimilar pipe arc welded joints, and which have the most significant influence on residual stresses?
- What is the most accurate heat source model for the prediction of pipe arc welding of dissimilar materials?

### 3. Material and method

The pipe was prepared and welded at the University of Miskolc, Miskolc, Hungary. Pipe welding with dissimilar material has been welded with MMAW process and with filler rods. A dissimilar pipe has an outer diameter of 133mm, with different thickness of 8 mm and 11, and a total length of 420 mm, as shown in **Figure 2**.

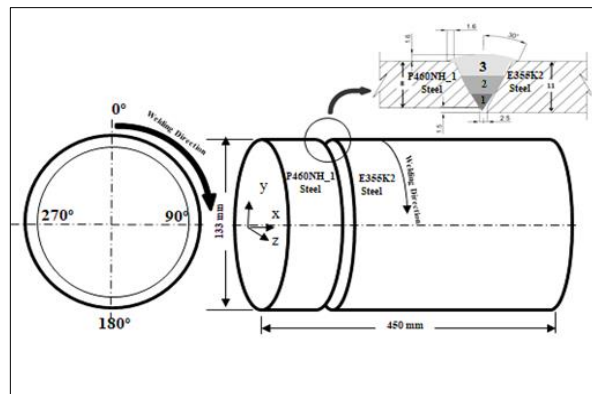


**Figure 2.** Schematic sketches of the welded pipe with the welding direction for three passes, dimensions in mm

The P460NH\_1 steel, E355K2 steel and the filler (A5.1-04: E6010) for the first pass and the second and third passes (A5.5-96: E6010) were selected respectively as the material for the welding pipe. The chemical compositions for the parent and weld materials, shown in **Table 2**. The pipe was joined with a manual circumferential weld. Welding parameters utilized in this study are given in **Table 3**. Usually, the welding efficiency is used between 65 and 88%.

**Table 2.** Chemical composition (wt%)

Materials	C	S	P	Mn	Si	Mo	Ni	Nb	V	Cr	Cu	Fe
P460NH_1 (BM-1)	0.2	0.001	0.02	1.4	0.33	0.1	0.01	0.05	0.2	0.01	0.03	95.23
E355K2 (BM-2)	0.1	0.01	0.86	0.8	0.01	-	-	0.02	0.058	0.02	0.02	-
Filler metal A5.1-04: E6010	0.1	-	0.02	0.4	0.14	0.5	0.15	-	-	0.1	0.17	-
Filler metal A5.5-96: E6010	0.1	0.01	0.01	0.63	0.36	0.01	0.02	-	-	0.03	-	-

**Table 3.** Welding parameters and heat source

Pass No.	Current (A)	Voltage (V)	Speed mm/s	Efficiency	Welding pool parameters			
					2a (mm)	b (mm)	c <sub>f</sub> (mm)	c <sub>r</sub> (mm)
1	80	23.2	2	0.8	5.6	4	5.3	8.3
2	90	23.6	2	0.8	11.5	3.8	5.2	8.3
3	100	24	2	0.8	13.8	4.7	5.3	8.2

### 5.1 X-ray-Diffraction measurement

X-ray diffraction is the most important non-destructive method to determine and analyse residual stress fields within crystalline materials in the welding pipe and other components. The X-ray method does not measure stress directly but measures strain from which residual stress values are calculated. The principle is simple. The XRD technique uses the distance between measuring the inter-atomic lattice spacing, i.e. d-spacing, like an atomic strain gauge.

**Figure 5** shows the basic principle of XRD. The residual stresses were measured at the post-processed surface using X-ray diffraction with equipment from Stresstech, XStress Robot X-ray Diffractometer as shown in **Figure 6 (a)** and **(b)**.

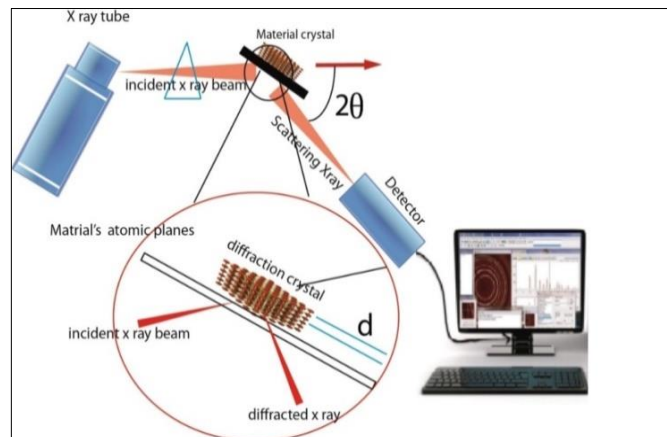


**Figure 5.** Schematic diagram of the basic principle of XRD

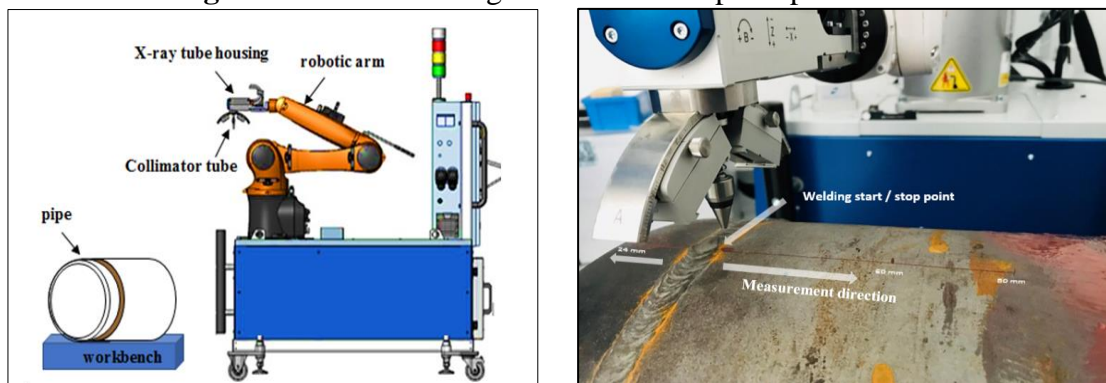


**Figure 6.** The examined positions of residual stress measurements by X-ray diffraction: (a) Xstress Robot XRD measurement (b) Close-up of the setup and measurement directions

## 5.2 Numerical simulation procedure

Flow chart of the procedure for the 2-D FE model calculation is shown in **Figure 7**. Complex numerical approaches are required to accurately model the welding process in 2-D, with finer mesh (small element size) and materials region used to simulate welding instead of 3-D to save the CUP time of computation.

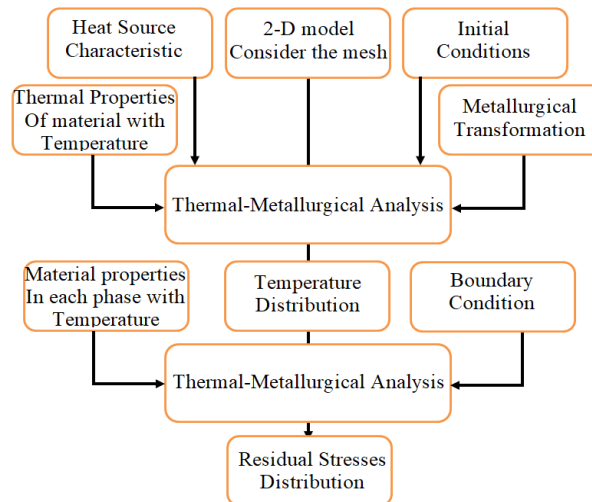


**Figure 7.** Flow chart of the welding simulation procedure

## 5.3 Two-dimensional Model (2-D) and three-dimensional Model (3-D)

**Figure 8** shows the 2-D model and 3-D model. The X-axis is pipe length direction, Y-axis is pipe thickness direction, and the Z-axis is pipe welding direction. The dimensions of the finite element model are the same as those of the experimental specimen

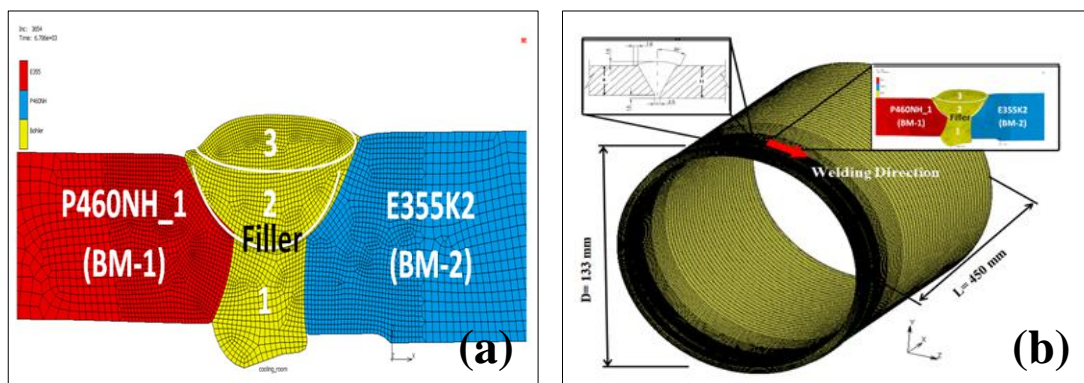


**Figure 8.** (a) 2-D model (b) 3-D model

## 4. Scientific result and claims

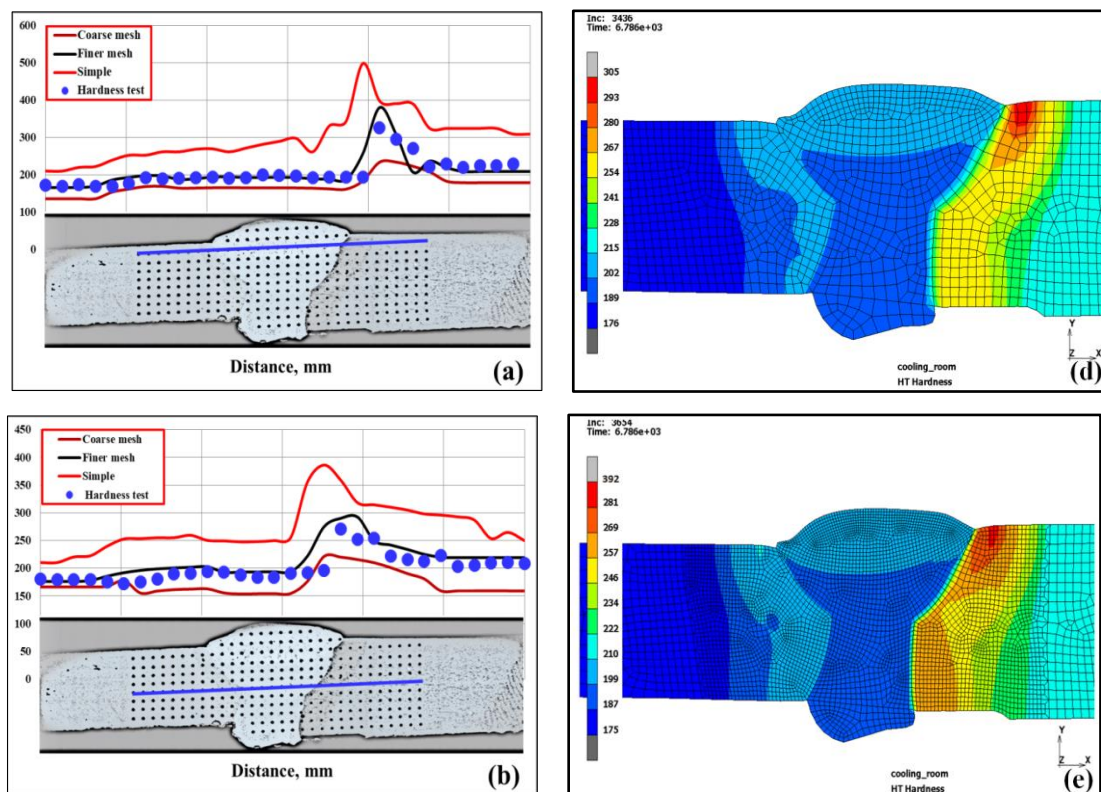
New scientific result of my dissertation can be summarized as follows:

## Claim 1:

A complex method was designed to validate the finite-element model for the process of manual arc welding of a pipe with dissimilar steels P460NH\_1 steel, E355K2 steel and the fillers for the first pass (A5.1-04: E6010) and the second and third passes (A5.5-96: E6010) were welded. I established a method for validation using hardness data and optical metallographic analysis of the heat-affected zone and the fusion zone. The area of the modelled weld-bead joint shape geometry is changed in multi-step iterative calculations to minimize the difference between the calculated and the measured hardness data and to create similarity of the phases identified by metallurgical optical measurement. The area of the weld-bead joint applied in computations varies between the values of the optically measured minimum and maximum area. Predicted results show good agreement with experimental results.

### a) Validation of Numerical simulation model using hardness test

Figure 9 shows three models (simple shape, coarse mesh and finer mesh model) that were used to compare with the hardness measurement. The predicted (finer mesh model) simulation results are shown to be in good agreement with the measurement results, meaning high accuracy.



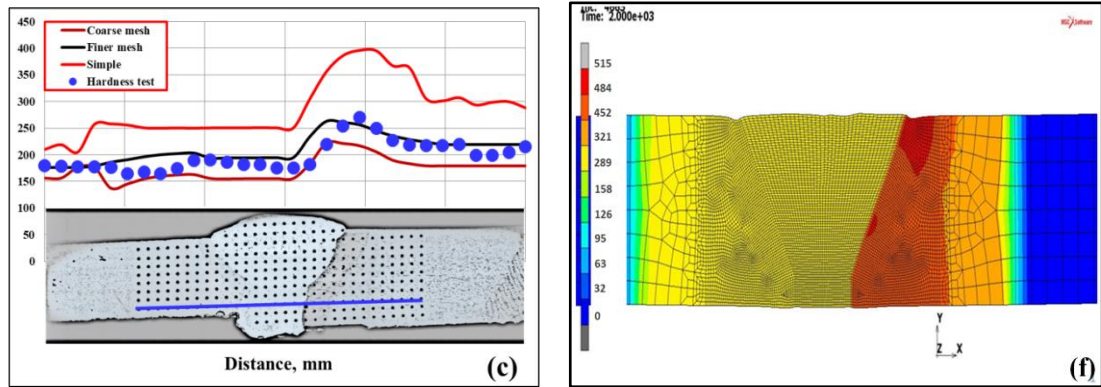


**Figure 9.** Three FEM models and comparison hardness test using (a) Finer mesh (b) Coarse mesh model (c) Simple model (d) Model with finer mesh (e) Model with coarse mesh (f) Simple model

The area of the weld-bead joint applied in computations varies between the values of the optically measured minimum and maximum area, as shown in **Figure 10**.

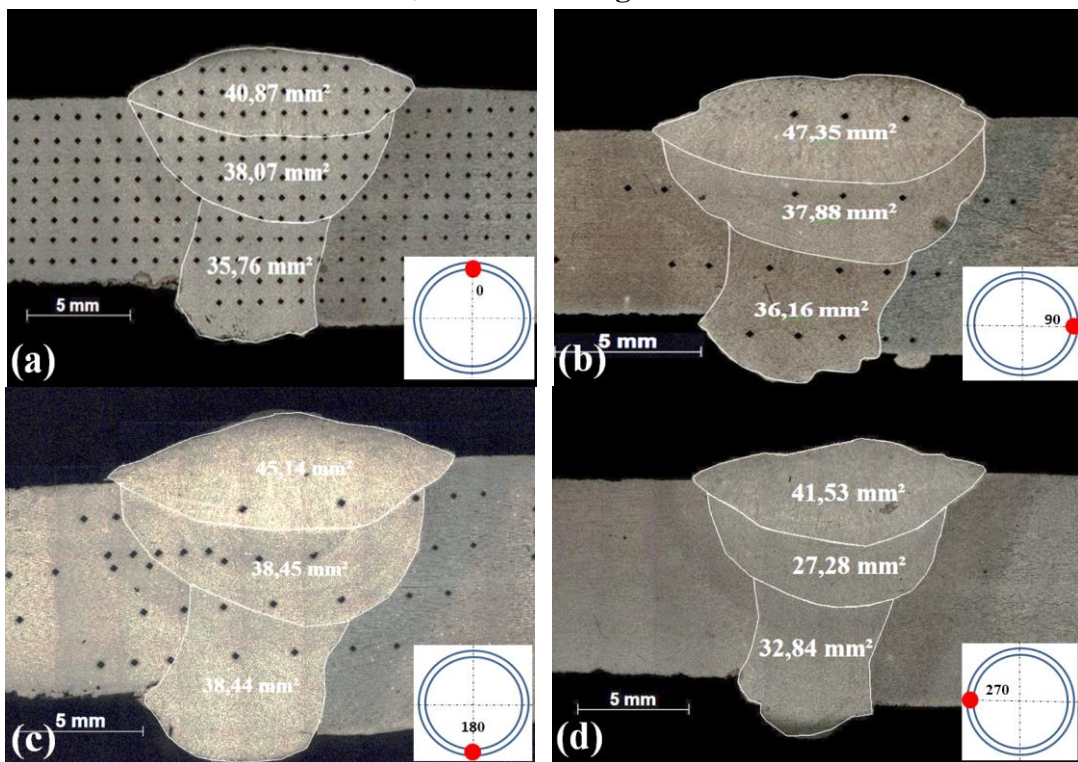


**Figure 10.** Weld bead profile at different position (a) 0° (b) 90° (c) 180° (d) 270°

**Figure 11** shows the comparison between the prediction and hardness test measurement and show good agreement.

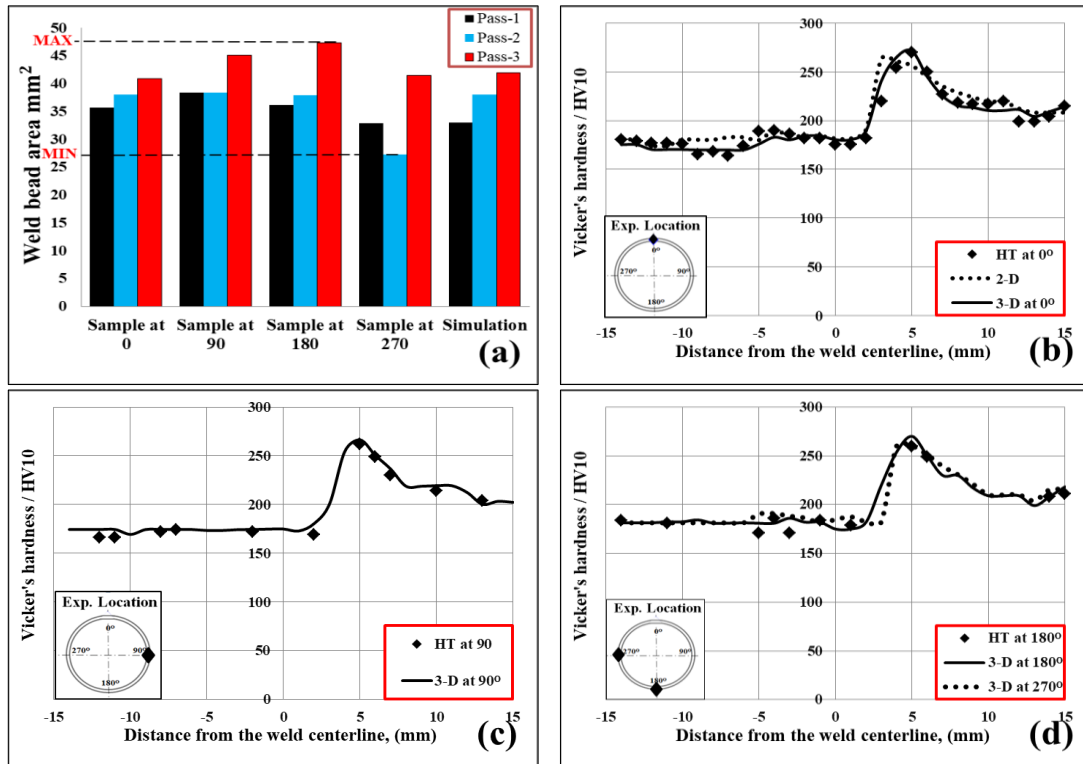


**Figure 11.** (a) Weld bead profile at different position with simulation (b) Comparison 2-D, 3-D with HT at  $0^{\circ}$  (c) 3-D with HT at  $90^{\circ}$  (d) 3-D with HT at  $180^{\circ}$  (e)  $270^{\circ}$

### b) Validation of Numerical simulation model using the distribution of phases

Microstructures of the welded joint, HAZ-1, HAZ-2, the base metal of dissimilar material and fusion zone are shown in **Figure 12**.

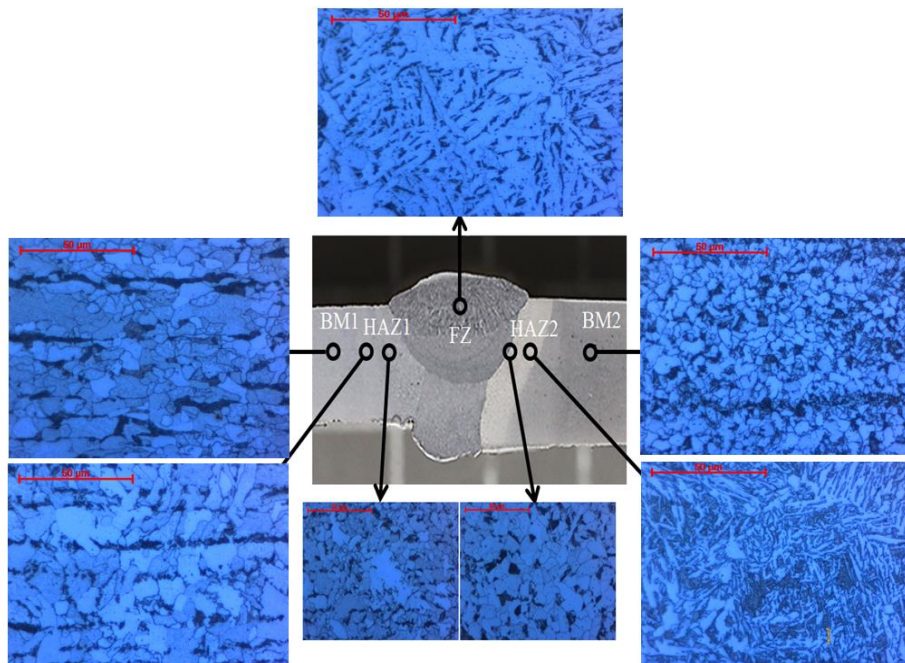


**Figure 12.** Microstructures of different areas of the welded structure

**Figure 13** shows the predicted microstructure constituent distributions in the simulated weld specimen. The distribution of the phases, which it is possible to calculate, gives information about



the dissimilar welding material that undergoes metallurgical changes due to the interaction of the welding.

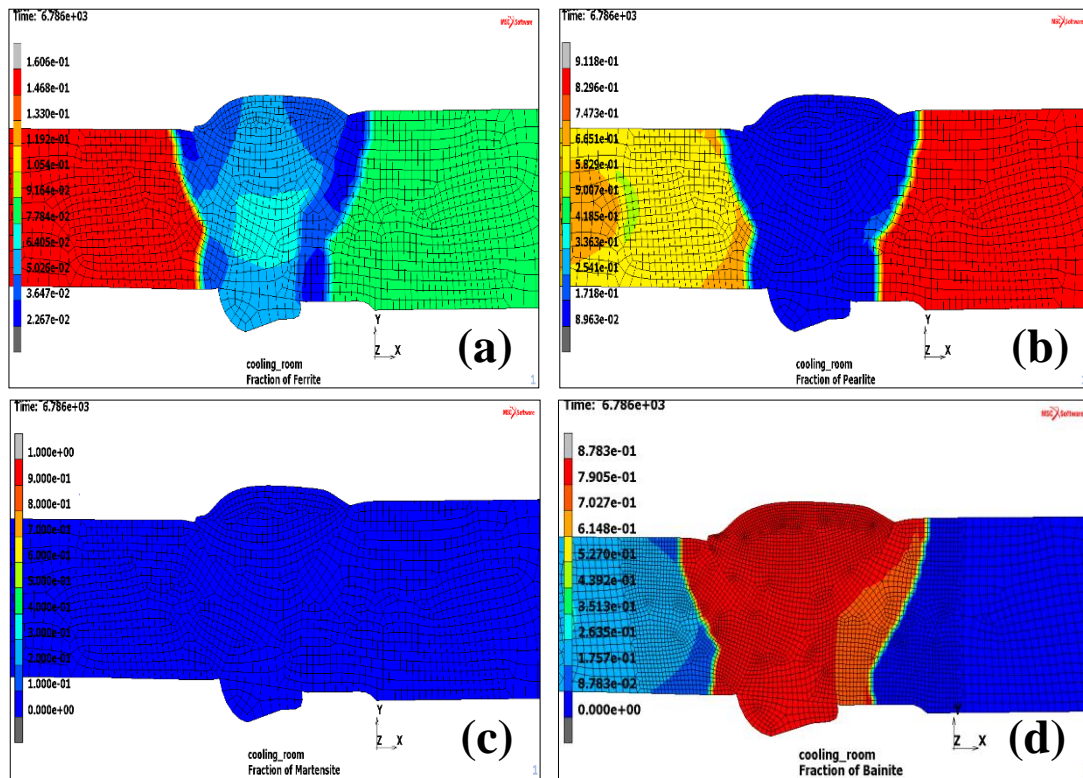


**Figure 13.** Distribution of (a) ferrite (b) pearlite (c) martensite (d) bainite phases of the simulation weld zone

### c) Validation of Numerical simulation model using the comparison of sectional morphology

From **Figure 14**, the double ellipsoid heat source models were used for all passes to successfully simulate the shape of full-penetration weld. Thus, it was verified that the heat source model was valid and could be used to simulate the weld morphology and temperature field accurately.

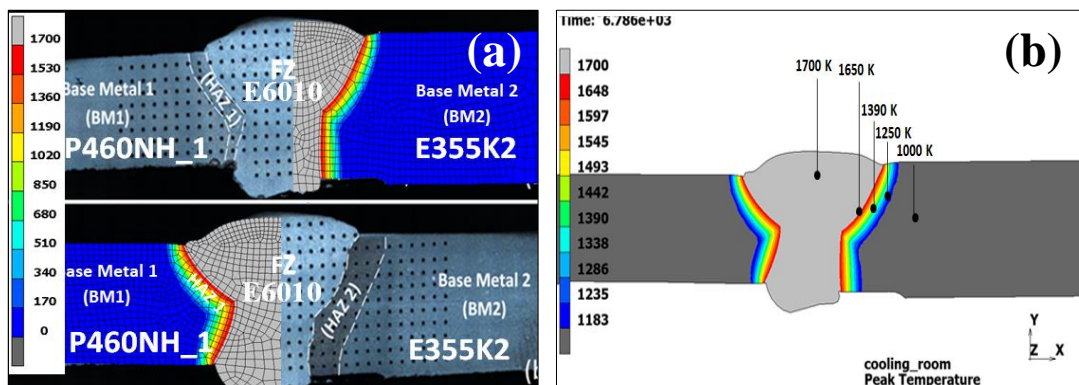


**Figure 14.** (a) Simulated temperature distributions in the cross-section (b) temperature profile in the dissimilar weld joint in [K]

#### d) Validation of Heat Source Model

The validation of the heat source model is done by observing the temperature histories of measured nodes and comparing the predicted and measured weld-pool shapes. The comparison between weld shape pool and heat source by the numerical model is presented in **Figure 15**.

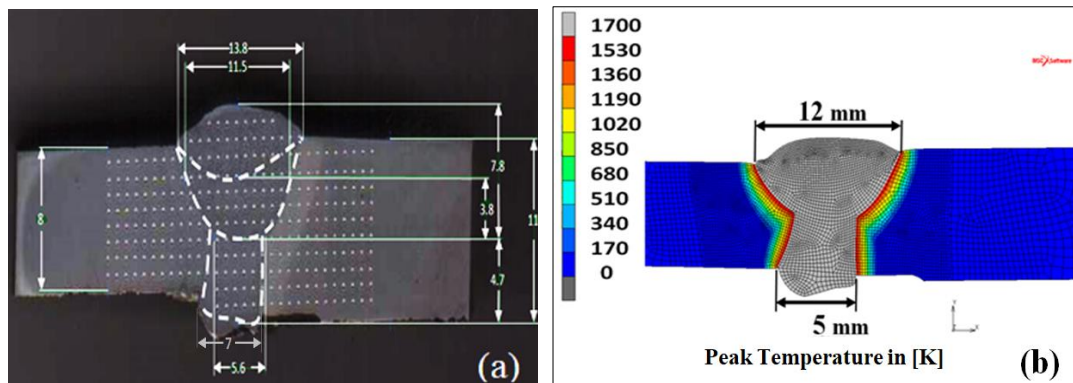


**Figure 15.** Weld pool profile obtained from (a) the specimen, (b) simulation, all dimensions in mm

#### Claim 2:

##### a) Comparison of residual stresses distribution for 3-D and 2-D models with XRD

I developed a two-dimensional (2-D) and three-dimensional (3-D) finite element model to simulate and predict the central angle-dependent welding residual stress distribution in a multi-pass girth-welded pipe model for the dissimilar steels (P460NH\_1 steel, E355K2 steel) and for the fillers used ((A5.1-04: E6010) for the first pass and the second and third passes (A5.5-96: E6010)). The 3-D model allows calculation results for axial and hoop residual stresses to be obtained with relatively good agreement to the measured data for both angles investigated. The comparison of calculated and measured data confirms that the 3-D model estimates the residual stresses more accurately than the 2-D model, even if the prediction of residual stresses is required at different angles around the longitudinal axis of the pipe welds. The angle dependency of residual stresses was observed by X-ray diffraction measurement for  $0^\circ$  and  $90^\circ$ , and the same trend was predicted by the 3-D finite-element model of pipe welding. This confirms that the only useful and permissible model to predict the residual stresses is the three dimensional one. Figures A-1 and A-2 show the comparison of axial and hoop residual stresses distribution for 3-D and 2-D models with XRD measurement on the outer surface. The measurement in depth is difficult to perform by X-ray diffraction or other means, but the 3-D model actually gives more extra information along the circumferential direction that can be considered as an alternative way to complete and describe the total stress state in the non-measurable parts of the heat-affected and the fusion zone. Calculation of the normalized root-mean-square deviation or error (NRMSD) is shown in **Table 4**, this table presents (NRMSD) between all models. It shows that 3-D is more accurate comparing with 2-D model.

**Table 4.** Calculation of the normalized root-mean-square deviation or error (NRMSD)

Model	Axial RS at 0° (NRMSD)	Axial RS 90° (NRMSD)	Hoop RS at 0° (NRMSD)	Hoop RS 90° (NRMSD)
2-D	1.987	-	2.090	-
3-D (5°)	1.839	-	1.459	-
3-D (90°)	1.096	1.963	3.781	2.192
3-D	1.2767	1.432	1.02	1.731

**Figure 16** presented the axial residual stress distribution at the positions of 0°/360° and 90° in 3-D pipe model along the outer surface path and compared with 2-D and XRD measurement. While the axial and hoop residual stresses were shown at all positions in **Figure 17**. However, both the hoop and axial residual stresses near start/end region (at 0°/360°) shown shape gradients and significantly different from those in 2-D model. A comparison of residual stress was also carried out between 2D/3D models under the conditions of the same peak temperature and the same heat source shape parameters. At the same time, a significant difference in stress values for those two models can be observed. However, this should not mean that the results of 2-D model were unacceptable.

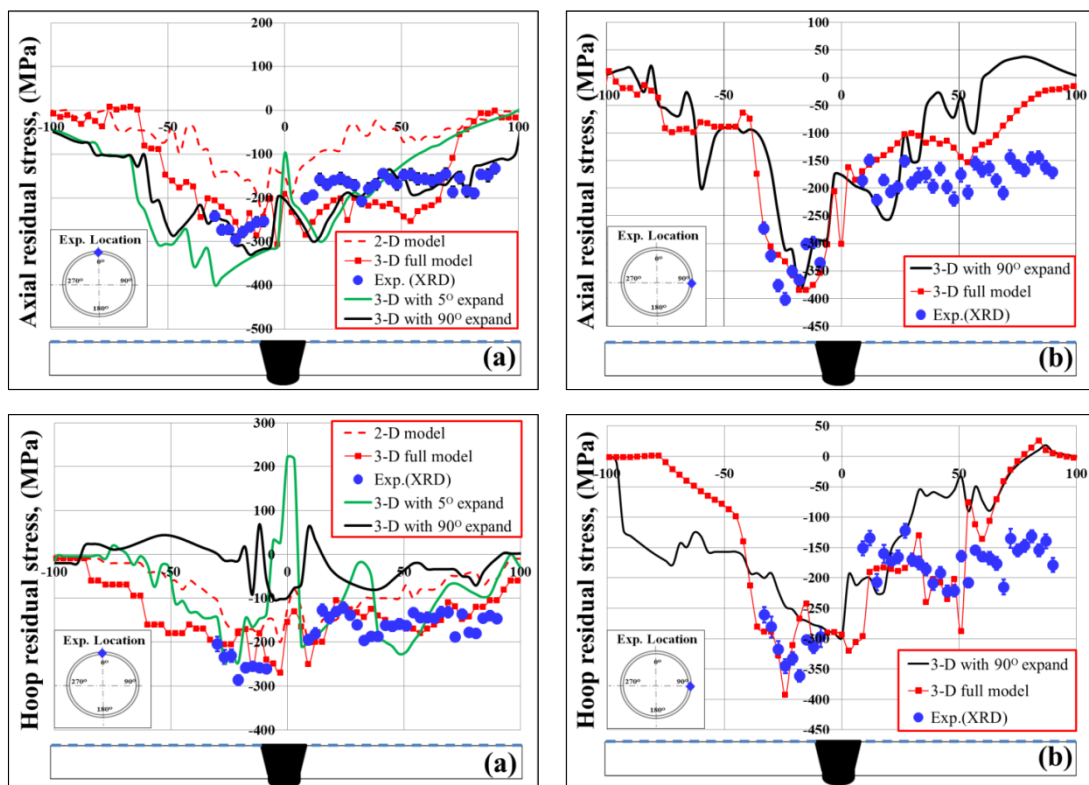


**Figure 16.** Comparison of axial and hoop residual stresses distribution for 3-D (5°, 90° expand and full) and 2-D models with XRD measurement on the outer surface: (a) predicted and measured RS distributions at 0°, (b) 3-D (5°, 90° expand and full) predicted and measured RS distributions at 90°

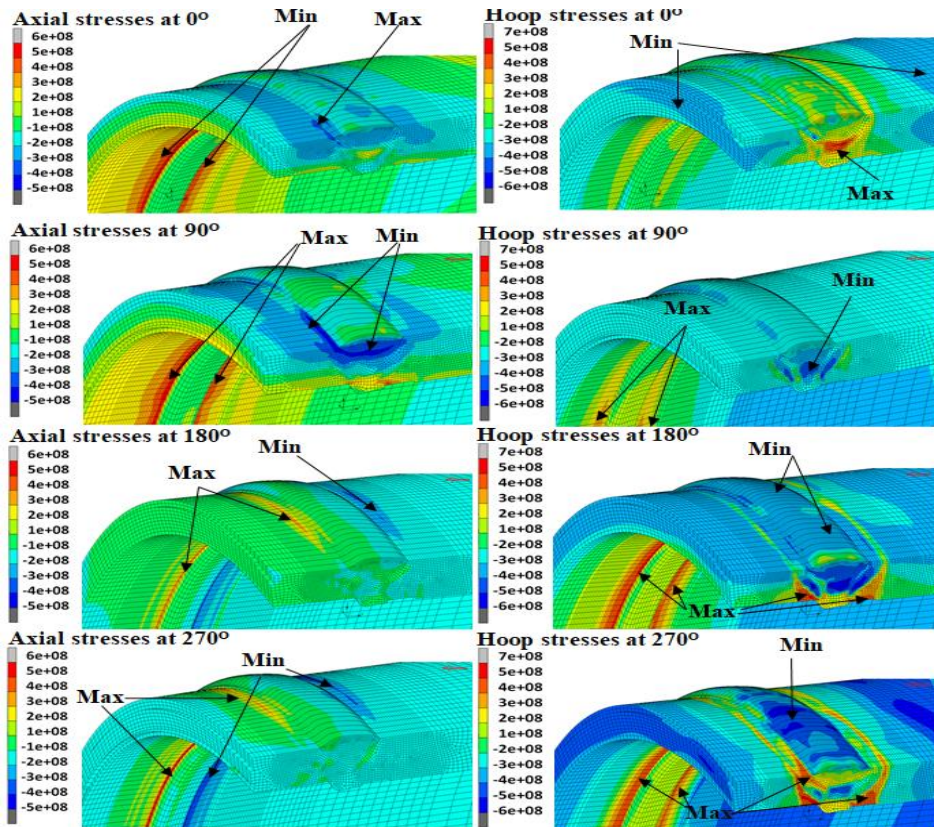


**Figure 17.** Axial and hoop residual stresses distributions with a cross-section of full 3-D model pipe weld at 0°, 90°, 180° and 270° [Pa]

### Claim 3:

For axial and hoop residual stresses in V-groove arc welding pipe with dissimilar material that used (P460NH\_1 steel, E355K2 steel) and for the fillers used ((A5.1-04: E6010) for the first pass and the second and third passes (A5.5-96: E6010)) distribution increases for the entire peak with almost the same heat input and current increase on the outer surface and through the thickness. However, the heat input and current have a relatively small effect on residual stresses on the inner surface. The axial residual stress distribution on the welded joint does not significantly change, but residual hoop stress shows some changes for both surfaces and through the thickness in case of weld speed effect. Although the number of passes is generally thought to have effect on residual stresses (fewer passes leading to higher stresses), the numerical results revealed that the hoop and axial stresses in the dissimilar welded joint do not change on the outer or inner surface related to the number of passes; two passes increase the residual stress distribution slightly in the middle of the weld. The root gap has no significant effect on residual stress distribution through the thickness and the outer and inner surface of weld dissimilar joints. In order to enhance the reliability of the joints, smaller heat input should be employed to decrease the residual stress.

## Claim 4:

**Figure 18** shows three-dimensional finite element simulation of the welding process, the applied heat source model is the combination of Goldak and conical types that provides a good agreement with the experimental results and the most accurate prediction for axial and hoop residual stresses in V-groove arc welding pipe with dissimilar material that used (P460NH\_1 steel, E355K2 steel) and for the fillers used ((A5.1-04: E6010) for the first pass and the second and third passes (A5.5-96: E6010)). Based on the results of the normalized root mean square error (NRMSE) implemented models analysis (**Table 5**), the minimum deviation was obtained by the combined model-independent on the circumferential angle (0 and 90 degrees) and the residual stress in the axial and circumferential directions.

**Table 5.** Calculation of the normalized root-mean-square deviation or error (NRMSD)

Heat source model	Axial RS at 0° (NRMSD)	Axial RS 90° (NRMSD)	Hoop RS at 0° (NRMSD)	Hoop RS 90° (NRMSD)
Gaussian	3.678	5.4	5.3	5.86
Goldak	1.2767	1.4322	1.02	1.731
Conical	4.8399	4.8019	5.677	3.64
Combined	0.3103	0.192	0.169	0.27

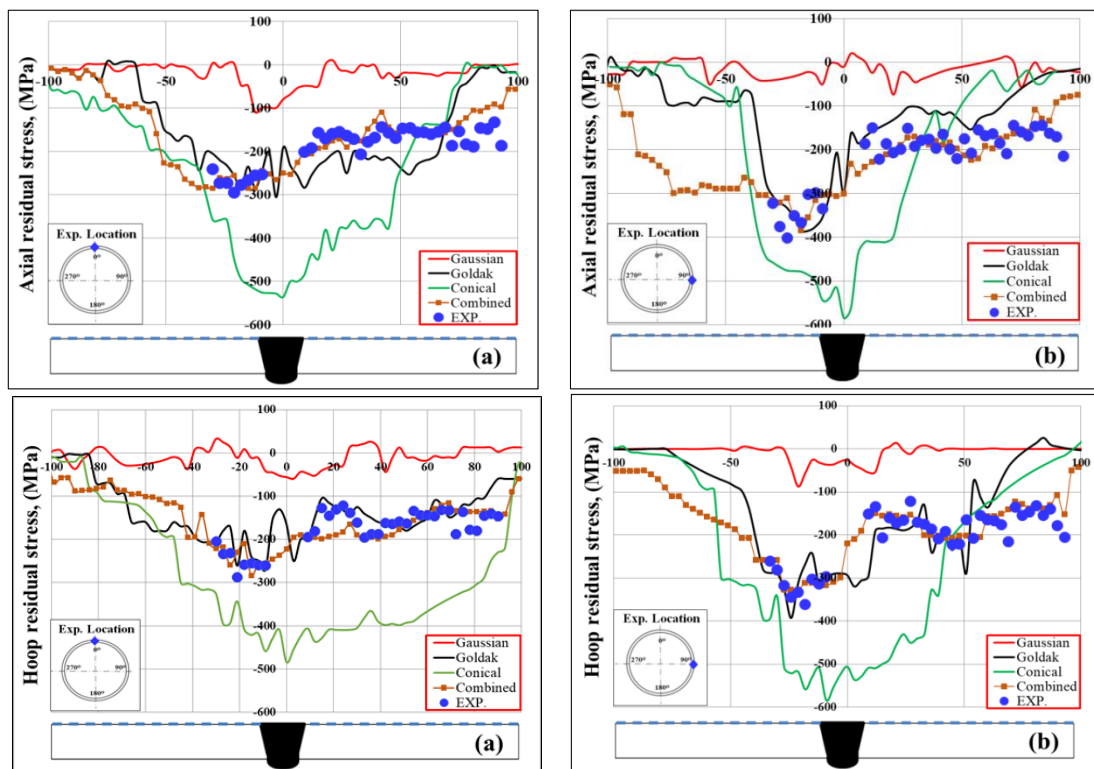


**Figure 18.** Comparison of axial and hoop residual stresses when using different heat source model with XRD measurements: Goldak; Gaussian; Conical; Combined heat source model (a) 0° (b) 90°

## 5. Future directions

Further parametric investigation of the significance of other problem variables requires researchers for residual stress to obtain adequate accuracy with different welding and techniques measurements. In addition, the interaction between phase transformation and residual stresses needs further investigation. Finally, more studies are required to make a guideline for designing a reasonable variable heat sources model in various multi-pass and one pass joints in future work.

### List of Author Publication

1. Alhafadhi, mahmood hasan, and Gyorgy krallics. "Simulation of the residual stress in a multi-pass oil and gas pipe weld joint." *journal of physics: conference series*. vol. 1527. No. 1. iop publishing, 2020.
2. Alhafadhi, mahmood hasan, and Gyorgy krallics. "Numerically simulated prediction of residual stresses in welding considering phase transformation effects." *journal of physics: conference series*. vol. 1527. no. 1. iop publishing, 2020.
3. Alhafadhi, mahmood, and György krállics. "Effect of the welding parameters on residual stresses in pipe weld using numerical simulation." *design of machines and structures* 10.1 (2020): 5-12.
4. Alhafadhi, mahmood hasan, and Gyorgy krallics. "The effect of heat input parameters on residual stress distribution by numerical simulation." *iop conference series: materials science and engineering*. vol. 613. no. 1. iop publishing, 2019.
5. Alhafadhi, mahmood hasan, and Gyorgy krallics. "Numerical simulation prediction and validation of two-dimensional model weld pipe." *machines. Technologies. Materials*. 13.10 (2019): 447-450.
6. Alhafadhi, mahmood hasan, and Gyorgy krallics. "Prediction and numerical simulation of residual stress in multi-pass pipe welds", (2021)
7. Mahmoodalhafadhi, Gyorgy Krallics, and Máté szűcs. "Finite element analysis on the formation of residual stresses during welding of oil and gas pipe."

### List of Author Conferences

1. Alhafadhi, mahmood hasan, and Gyorgy krallics. "Simulation of the residual stress in a multi-pass oil and gas pipe weld joint". *Journal of physics: conference series*. vol. 1527. No. 1. iop publishing, 2020.
2. Alhafadhi, mahmood hasan, and Gyorgy krallics. "The effect of heat input parameters on residual stress distribution by FEM". hungarian academy of sciences, Miskolc academic committee erzsébet square, miskolc, 3530.
3. Alhafadhi, mahmood hasan, and Gyorgy krallics. "The effect of heat input parameters on residual stress distribution by numerical simulation". 5th international conference on competitive materials and technological processes (ic-cmtp5)
4. Alhafadhi, mahmood hasan, and Gyorgy krallics "Analysis of residual stress during welding oil and gas pipe". *MultiScience - XXXII. MicroCAD International Multidisciplinary Scientific Conference* 2018.
5. Alhafadhi, mahmood, and György krállics. "Effect of the welding parameters on residual stresses in pipe weld using numerical simulation." *design of machines and structures* 10.1 (2020): 5-12.